

## Optimization techniques for mortars with self-compacting characteristics through Central Composite Design

Stéphanie Rocha<sup>1</sup>, Lino Maia<sup>2,3</sup>

<sup>1</sup>CONSTRUCT-LABEST, Faculty of Engineering (FEUP), University of Porto, Dr. Roberto Frias Street, 4200-465 PORTO, Portugal ([up202010607@g.uporto.pt](mailto:up202010607@g.uporto.pt)) ORCID 0000-0002-0984-4897

<sup>2</sup>CONSTRUCT-LABEST, Faculty of Engineering (FEUP), University of Porto, Dr. Roberto Frias Street, 4200-465 PORTO, Portugal ([linomaia@fe.up.pt](mailto:linomaia@fe.up.pt)) ORCID 0000-0002-6371-0179




<sup>3</sup>Faculty of Exact Sciences and Engineering, University of Madeira, Campus da Penteadá, 9020-105 Funchal, Portugal ([linomaia@fe.up.pt](mailto:linomaia@fe.up.pt)) ORCID 0000-0002-6371-0179

### Abstract

The high demand for concrete in civil construction promotes investment by researchers and builders to find methodologies that improve performance, costs and reduced environmental degradation. What justifies the large consumption of concrete is the possibility of improving its characteristics according to use. Self-compacting concrete offers a mixture with high flowability, compaction and good mechanical properties. Statistics tools can be used for better optimization of mixtures, such as the Design of Experiments (DoE). Therefore, the objective of this research was to optimize an experimental dataset of high strength self-compacting mortars using the Response Surface Methodology (RSM) for a Central Composite Design (CCD). The results showed a strong correlation between the D-Flow and T-funnel response factors, when compared with CS14h and CS28d models. The input variable w/c was the most significant. Numerical optimization showed good accuracy and compliance for low cost and environmental impact, maintaining high performance in fresh and hardened properties.

**Author Keywords.** Design of Experiments, Response Surface Methodology, Optimization of Materials, Construction Materials, Binding Materials

**Type:** Research Article

 Open Access  Peer Reviewed  CC BY

### Introduction

The role that concrete has in buildings and infrastructure constructions around the world is unquestionable, due to the versatility of application. The materials used to make concrete, such as cement, fine and coarse aggregate, are mostly generated from natural resources, which intensifies environmental exploitation (Ali et al. 2023).

In the 1980s in Japan, with a high growth in civil construction and the lack of skilled labor, buildings with concrete failures were frequent. These problems occurred mainly in the consolidation process, due to the characteristics of local structures, such as the slenderness of the pieces and the high rates of reinforcement, in view of a structural design capable of reducing high buckling and bending stresses caused by frequent earthquakes (Nunes 2001; Moraes 2010).

Local researchers and builders developed methodologies that would improve the quality of concrete, and a good configuration was to dismiss the consolidation process, promoting flow without an external force (Okamura 1997).

Therefore, self-compacting concrete is a mixture capable of flowing and compacting without the need for vibration, allowing the filling of formwork and reinforced structures by its own weight, without blockages or segregation. Unlike self-compacting concrete, traditional concrete needs to be vibrated to shape and fill the voids in the formwork (Day, R., Holton, I., Domone, P., & Bartos 2005). Brazilian standards NBR 15823 from 1 to 6 (2017) and European standards EN 206-1 (2007), NP EN 206-9 (2010) and NP EN 12350-8 to 12 (2010) are similar in terms of concept, classification and use of self-compacting concrete, except for the test methodology for determining segregation resistance.

Technological advances and the emergence of chemical additives, such as plasticizers and superplasticizers, which guarantee the fluidity of the mixture, the application of self-compacting concrete has improved even further (Aïtcin 2000).

To meet its properties, the dosage and choice of materials for the mixture must attend the following requirements: use a greater proportion of materials with fine-grained granulometry and cement; increasing viscosity, stability, filling voids and strength, the latter due to cement; and decrease the amount of coarse aggregates, to reduce the risk of segregation (Okamura, H.; Ouchi 2003).

However, this methodology increases the costs of the mixture, in addition to increasing properties such as shrinkage and cracking. Therefore, mixes with lower consumption of paste and fine aggregates should be proposed, so that the performance of the concrete is not compromised, mainly in terms of its rheological properties (Moraes 2010). Thus, it is necessary that studies be carried out to propose models that optimize the applicability of these mixtures, in order to determine the best compositions for a given purpose.

Currently, there is an increase in demand for complex concrete structures with varied geometries, requiring fluid and homogeneous concrete. Self-compacting concrete meets these requirements. However, care must be taken to characterize its properties in the fresh state. In addition, performance in the hardened state is directly related to the adjustments made to obtain the desired standards in the fresh state (Nuruzzaman et al. 2023; Zerbino et al. 2009).

An important statistical tool that can be applied to optimize the characterization of materials is the Design of Experiments (DoE). It is essential that this planning is done appropriately, that result found is not just data, making it possible to infer conclusions by the investigator (Neto, B. de B.; Scarminio, I. S.; Bruns 2001). There are countless benefits of using the DoE, such as reducing the number of experiments, the correlation between the addressed parameters, the definition of an optimal response within the investigated region and to building an empirical model with the parameters used and the responses found (Upasani, R.; Banga, S.; Ajay 2004). In the 1950s, an optimization technique based on factorial planes was created, applied when one wants to improve a response that depends on several factors, called Response Surface Methodology (RSM). It is currently used on a large scale, mainly in industrial processes (Box, G. E. P.; Wilson 1951; Box, G. E. P.; Hunzter, W. G.; Hunter 1978).

RSM aims to reach an excellent surface region, for what it repeats the modeling and displacement until it is reached. The models are usually fits of simple models, largely linear or quadratic, associated with factorial designs (Neto, B. de B.; Scarminio, I. S.; Bruns 2001).

Statistical models and optimization techniques for civil construction materials have been applied in several researches in recent years, such as the following works:

- In the replacement of coarse aggregates by pumice stone in concrete using RSM, analyzing the fresh and hardened properties, which resulted in a quadratic model and

an analysis of variance (ANOVA) with coefficient of determination ( $R^2$ ) above 99% and a fit error below 0.05 ( $<0.0001$ ), confirming a high accuracy of the model (Ali et al. 2023);

- In the application of foundry sand waste as a partial replacement of fine aggregate, using Design-Expert software for RSM and CCD tool for optimizing fresh and hardened properties. The fine aggregate was replaced at 0%, 10%, 20%, 30% and 40%. The performance at 20% was the best for mechanical properties, and 30% for fresh properties. The coefficient of determination ( $R^2$ ) ranged from 0.987 to 0.995, which corresponds to a high significance in the model. Thus, foundry sand is indicated to replace up to 20% of fine aggregate for conventional concrete and up to 30% for non-structural concrete, contributing to sustainable development (Ali et al. 2022);
- RSM to analyze the influence on the fresh and hardened properties of cementitious pastes when ordinary cement is replaced by irradiated polyethylene terephthalate (PET) waste and silica fume. The ANOVA models showed an error of less than 5%, allowing a good relationship between theoretical and experimental results (Khan et al. 2021);
- The use of RSM and sensitivity analysis to improve the heat transfer process of lightweight concrete hollow bricks. Conductivity, emissivity and recess size were used as input variables, and thermal transmittance as response variable. Finally, an optimized model based on RSM analysis was exposed, developing a quadratic polynomial model that solves nonlinear thermal problems. ANOVA ensured that the applied methodology was adequate for optimization (Del Coz Diaz et al. 2014);
- In the application of an RSM capable of predicting the workability of ultra-high performance self-compacting concrete reinforced with hybrid steel fibers. The study enabled a numerical optimization capable of finding a mixture with the highest flexural strength and the lowest amount of steel fibers (1.75% of microfiber volume) (Ghafari, Costa, and Júlio 2014).

In addition to the studies discussed above, in the last 15 years, several other works in planning experiments with civil construction materials have been carried out, in order to find the best optimization either by performance or sustainability parameters (Mohammed et al. 2012; Nunes et al. 2013; Keleştemur et al. 2014; Ferdosian and Camões 2017; Mermerdaş et al. 2017; Zahid et al. 2018; Matos et al. 2018; Imran Khan et al. 2020; Al Salaheen, M.; Alaloul, W.S.; Malkawi, A.B.; de Brito, J.; Alzubi, K.M.; Al-Sabaei, A.M.; Alnarabiji 2022; Shi et al. 2022; Anurag and Singh 2022; Waqar et al. 2023).

Therefore, the objective of this research is to optimize a set of experimental data of self-compacting high strength mortars, through statistical analysis and model adjustments, using the response surface methodology (RSM) for a central composite design (CCD). This methodology allows evaluating the statistical models developed by analysis of variance (ANOVA).

In the next topics, the database applied and how it was obtained (Maia 2022), and the criteria established for performance, adjustments and adaptations of the models were presented.

## **1. Experimental Program**

### **1.1. Experimental Database**

The research consists in evaluating 30 mixtures of high resistance mortar with self-compacting properties. The dataset was from a published study (Maia 2022). In this study, 4 independent quantitative variables were considered, namely:  $w/c$  = ratio between water and cement;  $Sp/p$

= ratio between superplasticizer and powder; w/p = proportion between water and powder; and s/m = ratio between sand and mortar.

For the central composite design of 30 compositions, a factorial design with  $2^4$  (four factors on two levels) treatment combinations, 8 axial and 6 central runs was defined to evaluate the experimental error. The independent variables were evaluated at the following levels:  $-\infty$ , -1, 0, +1,  $+\infty$ , according to Table 1. The value of  $\infty$  was equal to 2 for a rotational design, where  $\infty$  is equal to  $n_F^{1/4}$  and  $n_F$  correspond to the number of points in the factorial part of the design.

Input Variables	-2	-1	0	+1	+2
$X_1$ : w/c	0.78741	0.84110	0.89478	0.94847	1.00216
$X_2$ : Sp/p	0.02069	0.02210	0.02351	0.02492	0.02633
$X_3$ : w/p	0.46929	0.50129	0.53328	0.56528	0.59728
$X_4$ : s/m	0.42240	0.45120	0.48000	0.50880	0.53760

**Table 1:** Equivalence of coded and real values.

Response variables were considered: flow diameter (D-flow), time funnel (T-funnel), compressive strength in 24 hours (CS24h), and compressive strength at 28 days (CS28d). Table 2 indicates the response variables, units of measurement and methodology or technical specification for carrying out the tests in laboratory:

Response Variables	Unit	Methodology/Standard
$Y_1$ : D-flow	mm	Okamura & Ouchi (Okamura, H.; Ouchi 2003)
$Y_2$ : T-funnel	s	Okamura & Ouchi (Okamura, H.; Ouchi 2003)
$Y_3$ : CS24h	MPa	EN 196-1 (EN 2016)
$Y_4$ : CS28d	MPa	EN 196-1 (EN 2016)

**Table 2:** Response variables.

Table 3 presents the coded input parameters and results referring to the response variables obtained by Maia (Maia 2022): (i) D-Flow, being an average of two orthogonal distances from the slump test; (ii) T-Funnel; (iii) CS24h, being an average of six compressive strength values at the age of 24 hours; and (iv) CS28d, being an average of four compressive strength values at the age of 28 days.

Std	Run	Space Type	Coded values				Results			
			$X_1$ : w/c	$X_2$ : Sp/p	$X_3$ : w/p	$X_4$ : s/m	$Y_1$ : D-Flow (mm)	$Y_2$ : T-funnel	$Y_3$ : CS24h	$Y_4$ : CS28d
1	4	Factorial	-1	-1	-1	-1	331.0	30.50	59.49068	108.49110
2	14	Factorial	1	-1	-1	-1	341.0	17.69	51.63669	106.14450
3	8	Factorial	-1	1	-1	-1	332.5	27.29	60.86560	110.62260
4	21	Factorial	1	1	-1	-1	348.0	16.25	52.16580	104.86770
5	25	Factorial	-1	-1	1	-1	340.0	18.34	54.52573	106.50510
6	10	Factorial	1	-1	1	-1	367.0	11.45	50.87757	106.77540
7	28	Factorial	-1	1	1	-1	334.5	27.50	52.87920	107.50710
8	5	Factorial	1	1	1	-1	364.0	16.13	59.57883	111.65390
9	18	Factorial	-1	-1	-1	1	305.5	60.25	54.63112	101.26080
10	22	Factorial	1	-1	-1	1	314.5	35.50	49.99811	97.89542
11	20	Factorial	-1	1	-1	1	376.0	12.07	52.30638	107.37600
12	23	Factorial	1	1	-1	1	318.0	34.03	52.36447	102.44590
13	15	Factorial	-1	-1	1	1	317.5	32.23	55.42865	104.20690

14	30	Factorial	1	-1	1	1	334.5	19.71	53.76437	102.53980
15	19	Factorial	-1	1	1	1	331.0	26.37	56.56464	103.77990
16	12	Factorial	1	1	1	1	331.5	22.41	52.19865	106.42200
17	11	Axial	-2	0	0	0	312.5	42.10	63.96522	107.72540
18	26	Axial	2	0	0	0	343.5	19.82	48.29289	98.64815
19	24	Axial	0	-2	0	0	327.0	26.47	56.23838	106.40360
20	3	Axial	0	2	0	0	332.5	22.85	55.34302	104.70170
21	6	Axial	0	0	-2	0	312.5	64.50	52.07207	101.48550
22	1	Axial	0	0	2	0	357.5	15.18	55.76997	103.74990
23	27	Axial	0	0	0	-2	366.0	14.25	53.09370	102.38170
24	7	Axial	0	0	0	2	289.0	66.78	54.54092	101.05290
25	13	Center	0	0	0	0	352.0	18.28	55.74517	109.21820
26	9	Center	0	0	0	0	316.0	43.09	59.14607	103.12800
27	17	Center	0	0	0	0	326.5	35.44	59.99336	110.03500
28	29	Center	0	0	0	0	354.0	19.59	54.67565	106.64290
29	2	Center	0	0	0	0	331.5	23.00	56.80669	107.96340
30	16	Center	0	0	0	0	338.0	22.87	54.41940	107.09920

**Table 3:** Encoded values of input parameters and raw readings of results, performed by Maia (2022).

### 1.2. Development of the RSM model

For planning this experiment, the commercial software Design-Expert (version 13.0.13.0 64-bit, serial number: 0964-0841-3719-3394) was used, in which the polynomial regression model was developed. Central Composite Design (CCD) is the most practical Response Surface Methodology (RSM) as it includes three design points, as shown in Figure 1: (i) factorial points represented by two levels, with coded values of +1 and -1, with all possible combinations ( $2^k$  for a k-factor CCD); (ii) points present in the center of each face of the cube, called axial points (star points), located at a distance of  $-\infty$  and  $+\infty$  ( $2 \cdot k$ ); and, (iii) for central points, with zero value for the variables, located in the center of the cube (Stat-Ease 2014).

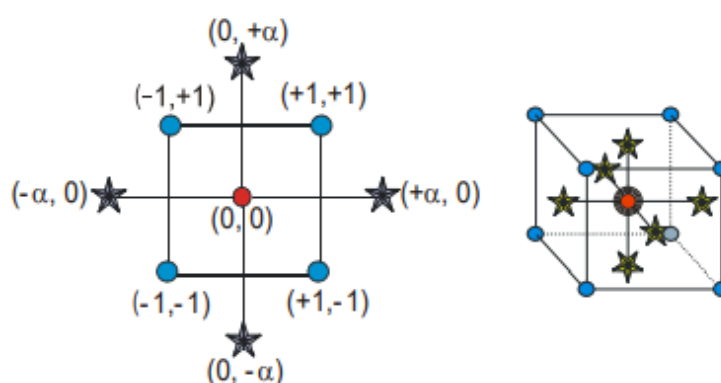


**Figure 1:** Design of factorial, axial and central points in the CCD (Stat-Ease 2014).

According to the design points and the experimental results, a second-order polynomial model can be related, according to the Formula 1 below:

$$Y = \beta_0 + \sum_{i=1}^k \beta_i X_i + \sum_{i=1}^k \beta_{ii} X_i^2 + \sum_{i < j} \beta_{ij} X_i X_j + \varepsilon \quad (1)$$

where  $Y$  is the response variable,  $\beta_0$  is the model intercept,  $\beta_i$  represents the linear coefficients,  $\beta_{ij}$  is the variable interaction coefficients,  $X_i$  and  $X_j$  are the design variables considered, and  $\epsilon$  is the fit error.

The models generated by the Design-Expert software allowed evaluating the following factors that were discussed in the next topics.

## 2. Discussion

### 2.1. Initial Considerations

Table 4 shows the statistical responses for the variables D-Flow, T-funnel, CS24h and CS28d of the 30 mixtures. The values found were: minimum, maximum, mean, standard deviation and coefficient of variation. All data found presented good adjustments and homogeneity, except for the T-funnel, which has a coefficient of variation (CV) of 52.32%.

Response	Name	Units	Minimum	Maximum	Mean	Std. Dev.	CV (%)
$Y_1$	d-flow	mm	289.00	376.00	334.83	19.96	5.96
$Y_2$	t-funnel	s	11.45	66.78	28.06	14.68	52.32
$Y_3$	CS24h	MPa	48.29	63.96	54.98	3.50	6.37
$Y_4$	CS28d	MPa	97.89	111.65	105.29	3.39	3.22

**Table 4:** Statistical responses of the 30 CCD points.

Before presenting the response modeling in RSM, it is interesting to evaluate the correlation of the response variables through simple scatterplots. Combinations between D-flow ( $Y_1$ ), T-funnel ( $Y_2$ ), CS24h ( $Y_3$ ) and CS28d ( $Y_4$ ) variables were performed in order to find the highest correlations between them.

The best correlation result is shown in Figure 2 (a) and (b), which are the T-funnel versus D-Flow and D-Flow versus T-funnel graphs, respectively. An exponential graphical trend is observed, with a strong downward correlation of -0.871.

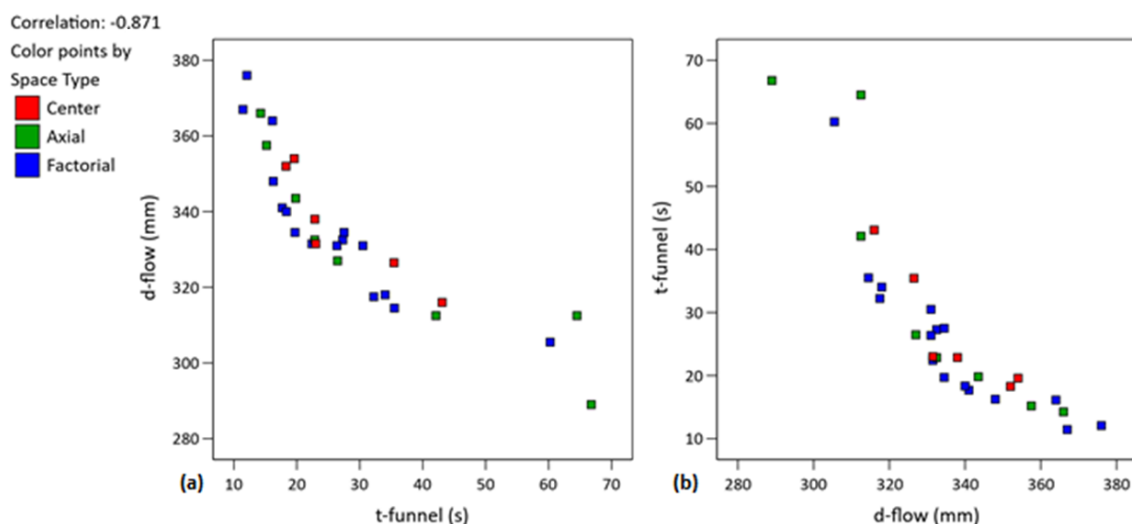


**Figure 2:** Correlation chart between (a) T-Funnel versus D-Flow and (b) D-Flow versus T-Funnel.

Figure 2 (a) and (b) corroborates with the literature referring to self-compacting concrete in relation to these two types of tests: T-Funnel and D-Flow are experiments to find properties in the fresh state for a free flow category of concrete, with the characteristic of filling a formwork under its own weight and segregation resistance (stability). In the placement stage of self-compacting concrete, a difference in flow and self-compacting capacity is observed, a

characteristic that justifies the replacement of conventional concrete by self-compacting in certain uses (Calado et al. 2015).

Figure 3 (a) and (b) shows the correlation between CS24h versus CS28d and CS28d versus CS24h, respectively. There is a moderate upward correlation trend of 0.597 with upward straight line trend. The other interactions between the response parameters have a weak correlation and were not presented in this discussion. Therefore, for an initial analysis, it is concluded that the relevant interactions occur between the properties in the fresh state (T-funnel and D-flow) and in the hardened state (CS24h and CS28d).

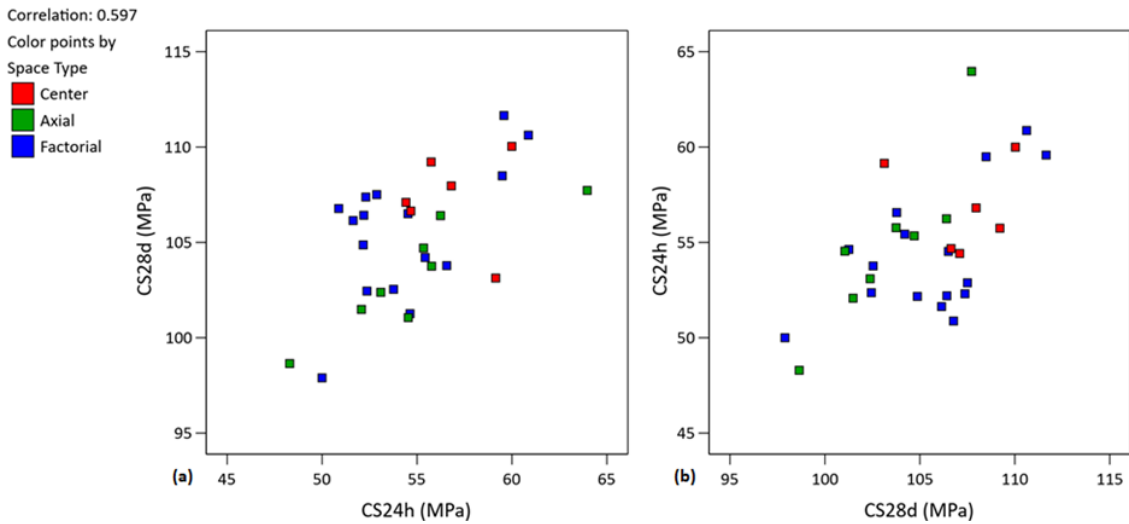


Figure 3: Correlation chart between (a) CS24h versus CS28d and (b) CS2.d versus CS24h.

### 2.2. D-flow Model

To define the polynomial model, important statistics were compared through regression analysis, such as “Square-R”, “p-value”, “f-value”, “Sum of Squares”, “standard deviation (sd)” and “PRESS”. Initially, the best model had a low value of adjusted  $R^2$  (0.3534) and predicted  $R^2$  (0.1765). In addition to being far from ideal values (close to 1.0), the relationship between the two variables was close to 20%. Therefore, it was evaluated through the normal plot of residuals, which is considered the most important diagnostic graph (Figure 4) that the point Std 11 Run 20 was misaligned with the others and was ignored in the model, thus performing a new analysis.

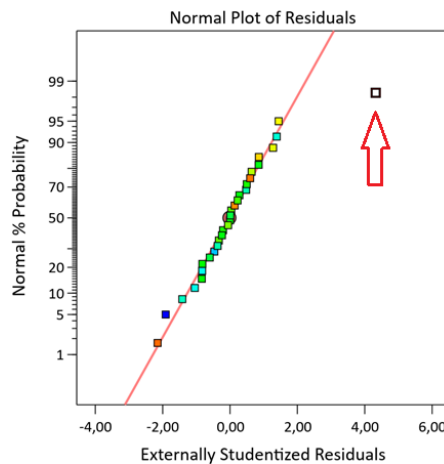


Figure 4: Plot normal probability of residuals for the D-flow model before adjustments.

In the subsequent analysis, the linear model was the one with the best result. In ANOVA, as observed in Table 5, it affirms the choice of the linear model, which presents a low “p-value” (<0.0001), below 0.05; and the “F-value” is 23.55, implying that the model is significant.

In order of relevance, factors  $X_4$  (s/m),  $X_3$  (w/p) and  $X_1$  (w/c) are the significant terms of the model, and dominant in relation to  $X_2$  (Sp/p) factor, which can be proven by the sum of squares values. The Lack of Fit presented a high “p-value” (0.9938) and an “f-value” of 0.2157 (above 0.05), which indicates that the lack of fit is not significant in relation to the pure error.

Source	Sum of Squares	Mean Square	F-value	p-value	Significance
<b>Model</b>	7811.22	1952.80	23.55	<b>&lt; 0.0001</b>	<b>significant</b>
w/c	<b>1386.15</b>	1386.15	16.71	0.0004	
Sp/p	17.33	17.33	0.21	0.6517	
w/p	<b>1883.58</b>	1883.58	22.71	< 0.0001	
s/m	<b>5078.17</b>	5078.17	61.23	< 0.0001	
<b>Residual</b>	1990.32	82.93			
Lack of Fit	896.49	47.18	<b>0.2157</b>	<b>0.9938</b>	<b>not significant</b>
Pure Error	1093.83	218.77			
<b>Cor Total</b>	9801.53				

**Table 5:** ANOVA for D-Flow response.

Table 6 presents the statistical values to increase the ANOVA. It is verified that the relationship between the adjusted  $R^2$  and the predicted  $R^2$  is within the 20% limit and with its maximum values for the linear model.

The term “Adeq Precision” measures the relationship between the signal and the fluid. Values above 4 are ideal. As its value is 17.2817, it suggests an adequate signal, again indicating that the model can be used to navigate the design space.

Std. Dev.	Mean	C.V.%	$R^2$	Ajusted $R^2$	Predicted $R^2$	Adeq Precision
9.11	333.41	2.73	0.7969	0.7631	0.7390	<u>17.2817</u>

**Table 6:** Fit statistics for D-Flow.

The factor coefficients coded D-flow are presented in **Table 7**. The input variables w/c, Sp/p, w/p and s/m are considered significant values and are multicollinear, because it present correlations above 1.

Factor	Coefficient Estimate	Standard Error	95% CI Low	95% CI High	VIF
Intercept	332.35	1.70	328.84	335.85	
w/c	7.80	1.91	3.86	11.73	1.01
Sp/p	0.87	1.91	-3.06	4.81	1.01
w/p	9.09	1.91	5.15	13.02	1.01
s/m	-14.92	1.91	-18.86	-10.98	1.01

**Table 7:** Coefficients for D-flow coded factors.

After adjusting the model, the normal probability graph of residuals was presented as can be observed in Figure 5 (a), which presents a better fit than the previous configuration, with the points close to the line, however, it appears to have a S shape, ideally linear or normal. For the residual versus run graph in Figure 5 (b), it was verified that the values obey the interval ( $\pm 3.54581$ ) and have random dispersion, with no upward or downward trend, which is considered ideal.



The residual versus predicted graph, as shown in Figure 5 (c), also has random dispersion and the points obey the established interval ( $\pm 3.54581$ ). And finally, Figure 5 (d) shows the predict versus actual graph, which demonstrates that the data are well correlated with the predicted values. In addition, the graph shows the location of the disregarded point (Std 11, Run 20) in the RSM.

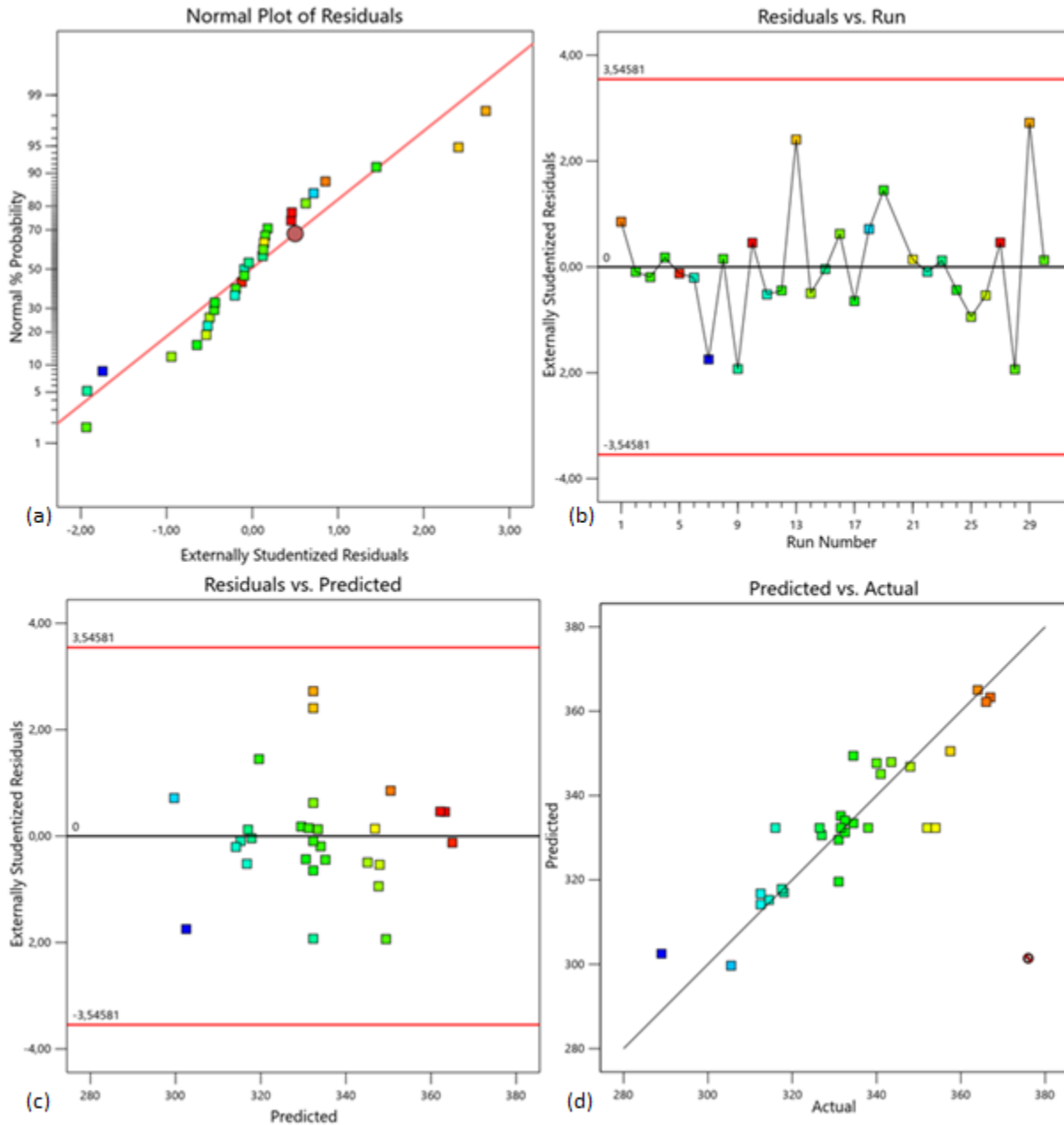


**Figure 5:** (a) Normal versus Residuals D-flow plot; (b) Residuals versus Run D-flow plot; (c) Residuals versus Predicted D-flow plot; e, (d) Predicted versus Actual D-flow plot.

### 2.3. T-funnel Model

In defining the polynomial model, through regression analysis, important statistics were compared. The best model for these inputs and outputs had an adjusted  $R^2$  value of 0.3976 and a predicted  $R^2$  of 0.2279, which represents a low significance, since ideally these values should be close to 1 and that the relationship between the adjusted and the predicted value is less than 20%. Therefore, in a preliminary investigation for adjusting this model, it was found

that the point Std 11 Run 20, in the same way as the analysis of the D-flow model, was located in a distant position from the others, as can be observed in Figure 6 (a).

In addition, the model suggested in Figure 6(b), through the Box-Cox plot, that the 95% confidence intervals for Lambda ( $\lambda$ ) are between -0.95 and 0.49, with the best  $\lambda$  being equal to -0.21. Therefore, an “inverse square root” transform was recommended so that  $\lambda$  is within the 95% confidence interval.

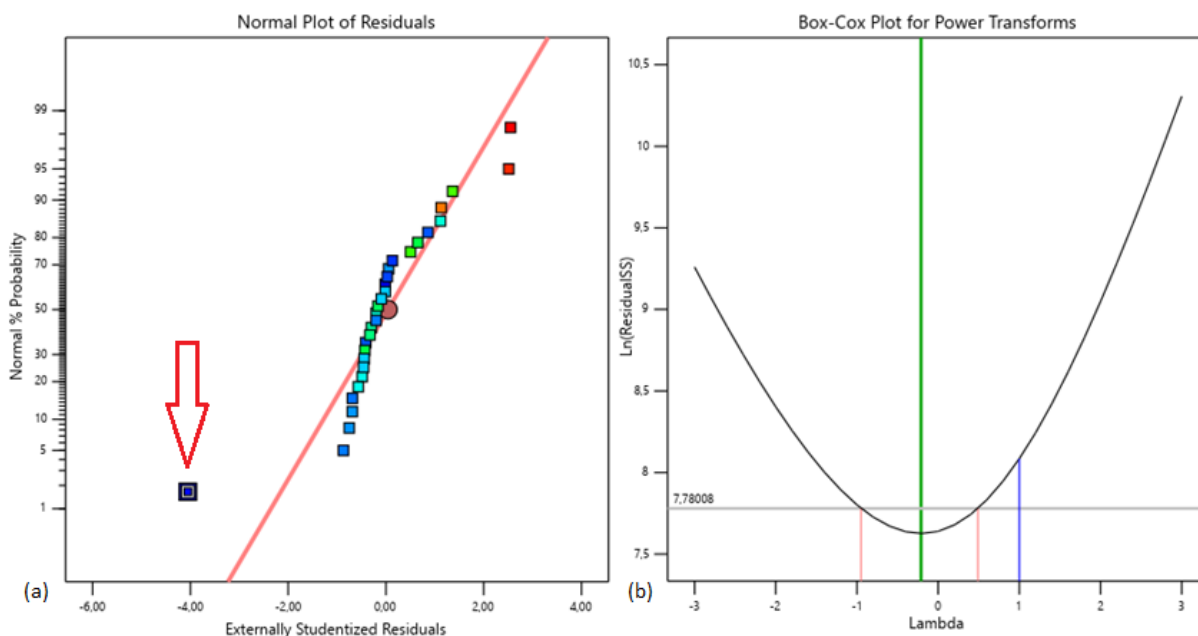


Figure 6: (a) Normal Plot; (b) Box-Cox plot.

After the adjustments, the model that presented the best result was the linear one. In Table 7, the T-funnel ANOVA shows the significant model, as it has a low “p-value” (<0.0001) and an “F-value” of 22.81. There is only a 0.01% chance that can a high F-value occur due to noise. Factors  $X_4$  (s/m),  $X_3$  (w/p) and  $X_1$  (w/c), in ascending order of relevance, are the significant terms of the model, and dominant in relation to factor  $X_2$  (Sp/p), since that this last entry is a non-significant term, as it has a “p-value” above 0.05 (0.7199). The lack of fit was insignificant, as it presented a “p-value” of 0.9806 and an “f-value” above 0.05 (0.2809). Therefore, relative to pure error, the lack of fit is not significant.

Source	Sum of Squares	Mean Square	F-value	p-value	Significance
<b>Model</b>	0.0414	0.0104	22.81	<b>&lt; 0.0001</b>	<b>significant</b>
w/c	<b>0.0111</b>	0.0111	24.48	< 0.0001	
Sp/p	0.0001	0.0001	0.13	0.7199	
w/p	<b>0.0139</b>	0.0139	30.68	< 0.0001	
s/m	<b>0.0203</b>	0.0203	44.68	< 0.0001	
<b>Residual</b>	0.0109	0.0005			
Lack of Fit	0.0056	0.0003	<b>0.2809</b>	<b>0.9806</b>	<b>not significant</b>
Pure Error	0.0053	0.0011			
<b>Cor Total</b>	0.0523				

Table 7: ANOVA for lineal model - T-Funnel.

In Table 8 the  $R^2$  is 79.17%, and the ratio between the adjusted  $R^2$  and the predicted  $R^2$  is less than 0.2. Also, the “Adeq Precision” has the value 17.3165, which is greater than 4, indicating that the signal is adequate and that it can be used to navigate the design space.

Std. Dev.	Mean	C.V.%	$R^2$	Ajusted $R^2$	Predicted $R^2$	Adeq Precision
0.0213	0.2018	10.56	0.7917	0.7570	0.7203	<u>17.3165</u>

**Table 8:** Fit statistics for T-funnel.

The estimated T-funnel coefficients are presented in Table 9, and are considered adjustments around the mean response of all runs, within the 95% confidence interval. Standard errors, confidence intervals and the Variance Inflation Factor (VIF) are also presented.

Factors  $X_1$ ,  $X_2$ ,  $X_3$  and  $X_4$  have VIF greater than 1.0, which indicates that these factors are multicollinear. It is noteworthy that values lower than 10 are tolerable.

Factor	Coefficient Estimate	Standard Error	95% CI Low	95% CI High	VIF
Intercept	0.1991	0.0040	0.1909	0.2073	
w/c	0.0221	0.0045	0.0129	0.0313	1.01
Sp/p	-0.0016	0.0045	-0.0108	0.0076	1.01
w/p	0.0247	0.0045	0.0155	0.0339	1.01
s/m	-0.0298	0.0045	-0.0390	-0.0206	1.01

**Table 9:** Coefficients in Terms of Coded Factors for T-funnel.

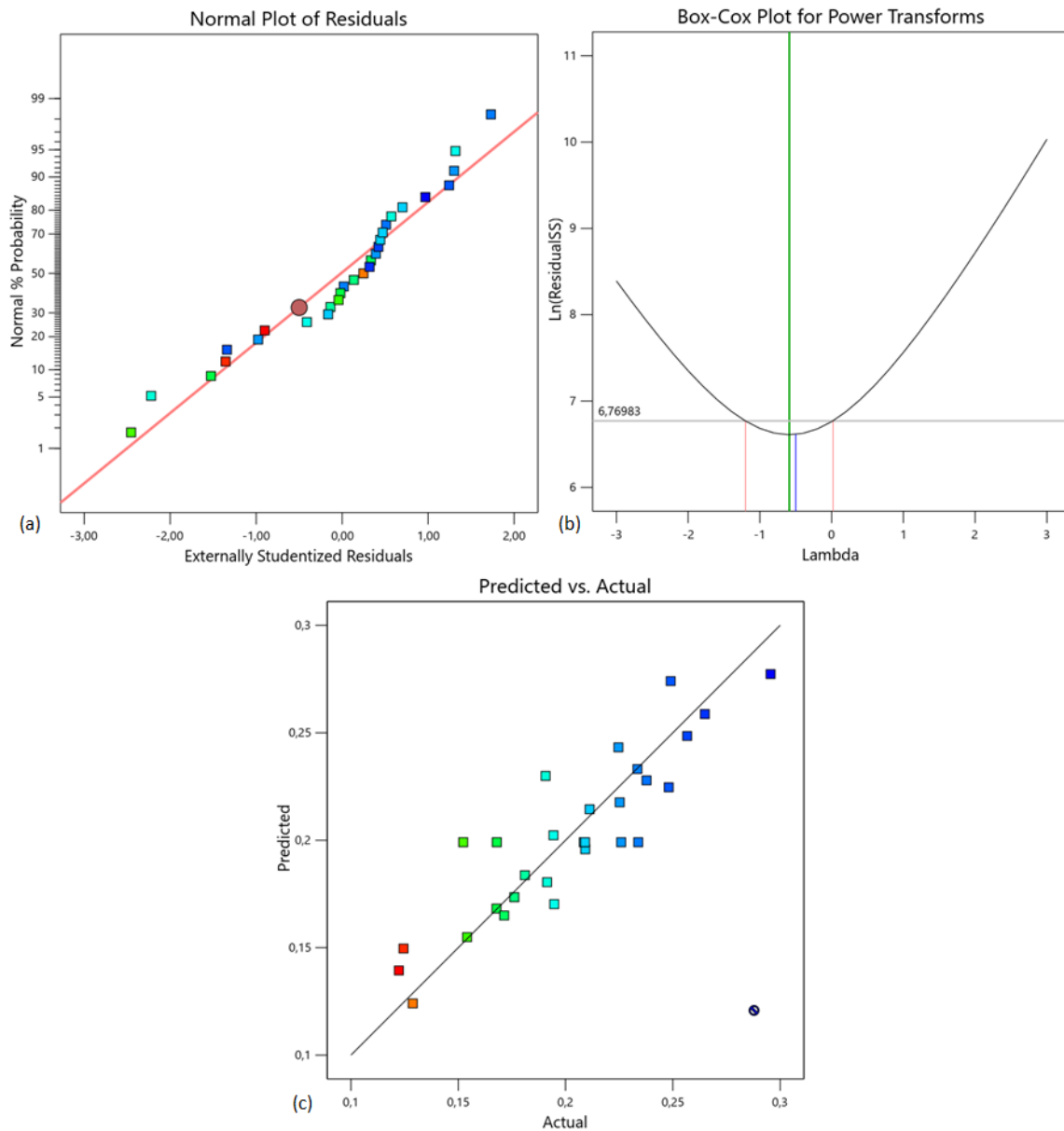


Figure 7 (a) shows the normal probability plot of the residuals after being adjusted ignoring the point Std 11 Run 20, and performing the “inverse square root” transformation. Although the points are close to a straight line, they have an S shape and it is recommended that it be

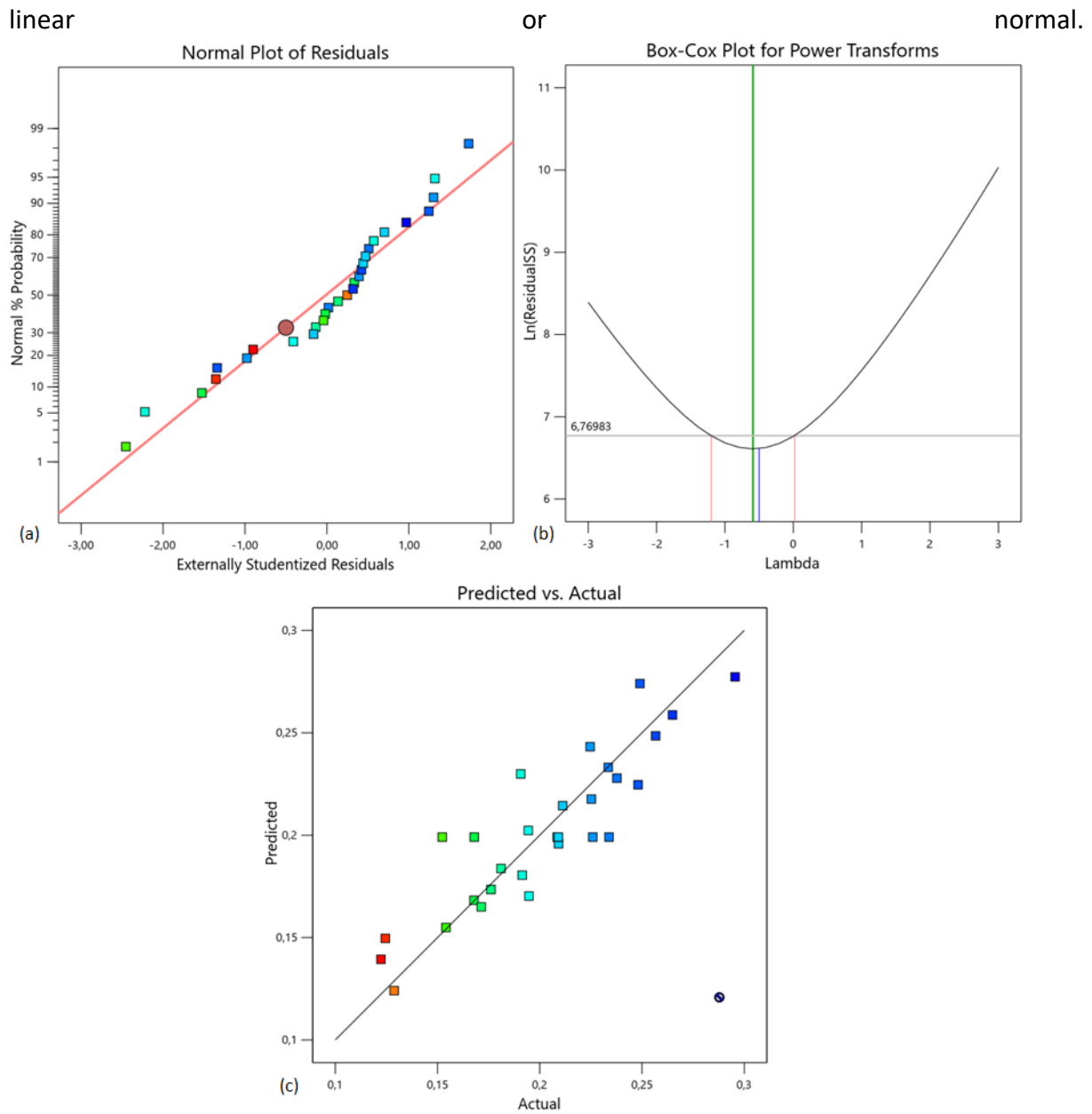


Figure 7 (b) shows the Box-Cox plot with the recommended transform, and the lambda ( $\lambda$ ) within the established range.

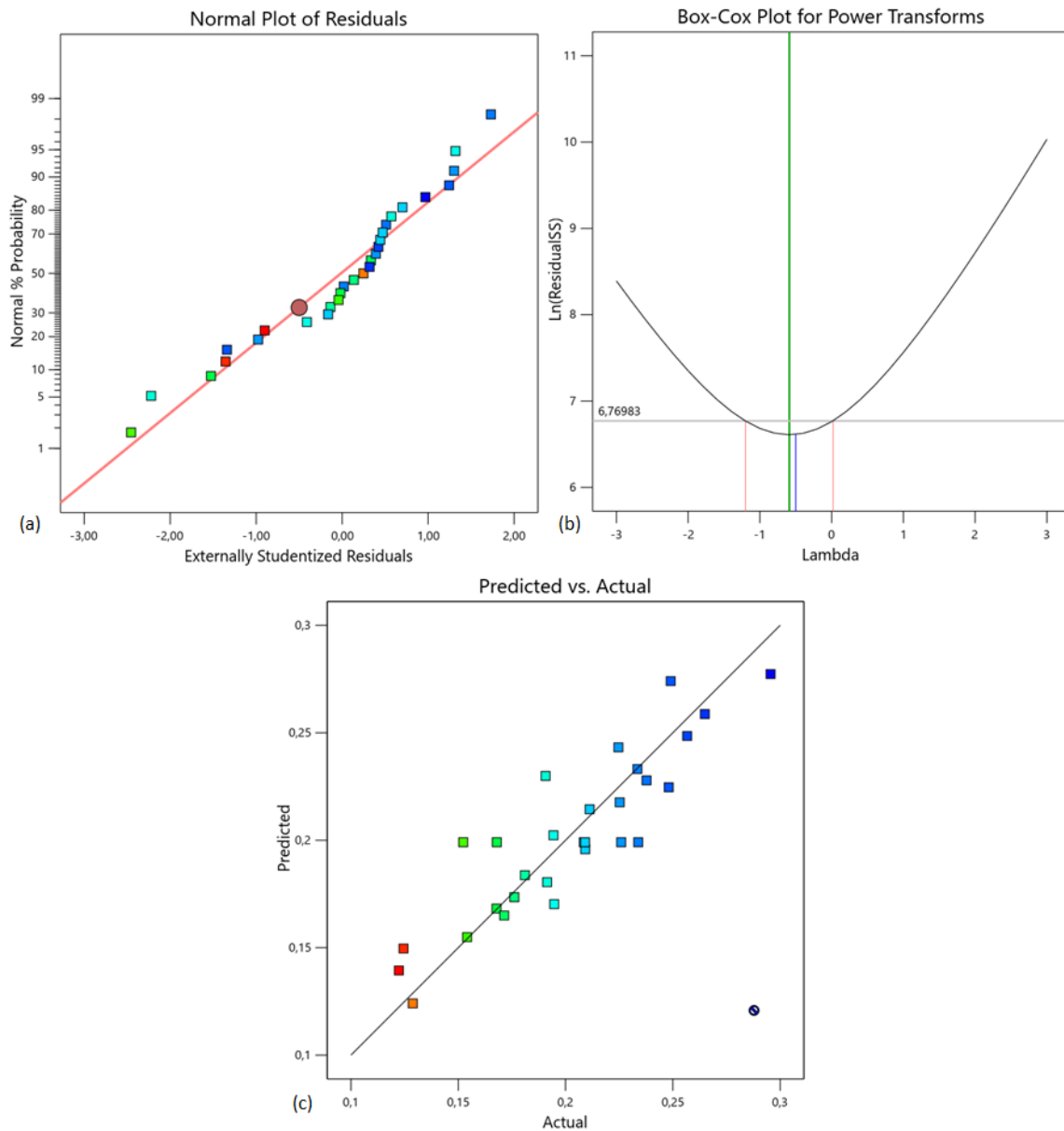


Figure 7 (c) shows the predicted versus actual graph, in which an inclined line is observed and with the points uniformly distributed around this line. Predicted and measured values vary between 85.12% and 130.73%. Despite the good distribution of the points, its present dispersions when compared with the D-flow data, for example. The location of Std 11 Run 20 point, which was disregarded for this analysis, is shown in the graph.

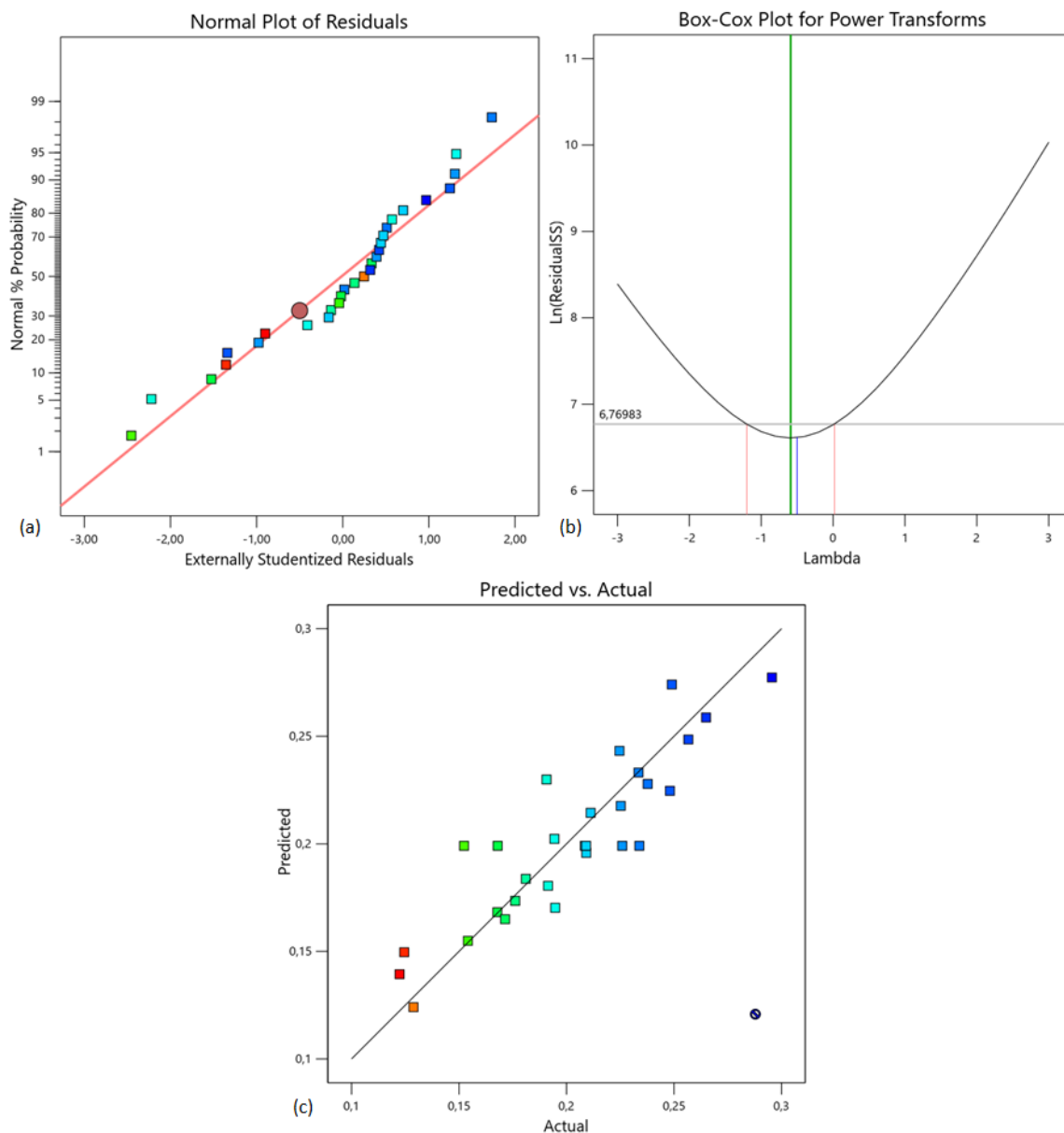


Figure 7: (a) Normal plot of residuals T-funnel; (b) Box-Cox plot for T-funnel transform; and, (c) Predicted versus Actual plot for T-funnel.

#### 2.4. Model for Compressive Strength with 24 hours (CS24h)

The Compressive Strength model with 24 hours (CS24h) was defined from linear regression. At first, the best model found was the linear one, with an adjusted  $R^2$  value of 0.2979 and a predicted  $R^2$  of 0.1193, therefore, far from 1.

No points were observed in the graph of the normal probability of residuals that disagreed with the considered profile. Therefore, none of the 30 response variable data for CS24h was disregarded.

ANOVA for the linear model is presented in Table 10. The “p-value” is 0.0112 (below 0.05), there is a 1.12% chance of an F-value occurs due to noise; and the “F-value” is 4.08, which implies that the model is significant. Only the term  $X_1$  (w/c) is significant, as it is the only one among the input variables that has a “p-value” less than 0.05. For the variables  $X_2$  (Sp/p),  $X_3$  (w/p) and  $X_4$  (s/m) the models are insignificant, and reducing these variables can be an alternative to improve the model.

The Lack of Fit (F-value) equal to 1.74 demonstrates that the value in relation to the pure error is not significant. There is a 28.22% chance of a misfit due to noise.

Source	Sum of Squares	Mean Square	F-value	p-value	Significance
<b>Model</b>	139.87	34.97	4.08	0.0112	significant
w/c	<b>128.12</b>	128.12	14.93	<b>0.0007</b>	
Sp/p	1.92	1.92	0.22	0.6407	
w/p	3.96	3.96	0.46	0.5029	
s/m	5.87	5.87	0.68	0.4160	
<b>Residual</b>	214.48	8.58			
Lack of Fit	187.49	9.37	1.74	0.2822	not significant
Pure Error	26.99	5.40			
<b>Cor Total</b>	354.36				

**Table 10:** ANOVA for CS24H.

In Table 11 as already mentioned, the value of  $R^2$  is 39.47% and a low value of predicted  $R^2$  (11.93%) and adjusted  $R^2$  (29.79%). However, the difference between the two is still less than 20%, which characterizes it as a reasonable agreement.

The signal-to-noise ratio is measured in “Adeq Precision”, which has a desirable ratio, that is, greater than 4, which indicates an adequate signal (7.7289).

Std. Dev.	Mean	C.V.%	$R^2$	Adjusted $R^2$	Predicted $R^2$	Adeq Precision
2.93	54.98	5.33	0.3947	0.2979	0.1193	<u>7.7289</u>

**Table 11:** Fit statistics for CS24h.

A Table 12 presents the estimated coefficients, standard errors, 95% confidence intervals and VIF. The estimated CS24h coefficients are the average response fits of the runs. The VIF de  $X_1$ ,  $X_2$ ,  $X_3$  and  $X_4$  is equal to 1.0. They are orthogonal factors and it is an acceptable result.

Factor	Coefficient Estimate	Standard Error	95% CI Low	95% CI High	VIF
Intercept	54.9800	0.5348	53.88	56.08	
w/c	-2.3100	0.5979	-3.54	-1.08	1.0000
Sp/p	0.2825	0.5979	-0.95	1.51	1.0000
w/p	0.4064	0.5979	-0.82	1.64	1.0000
s/m	-0.4946	0.5979	-1.73	0.74	1.0000

**Table 12:** Coefficients in Terms of Coded Factors – CS24h.



The residual normal probability plot for CS24h is shown in

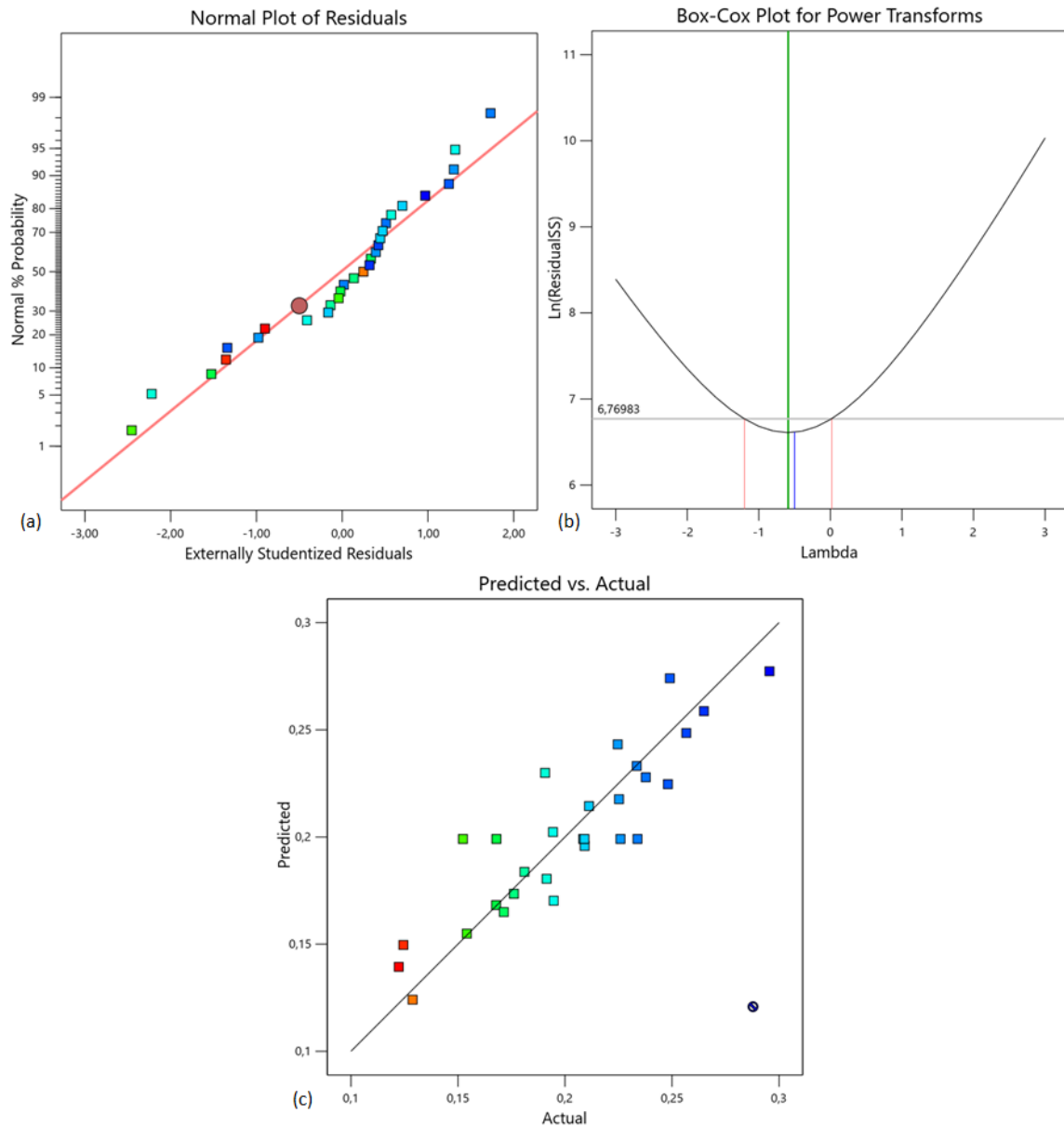
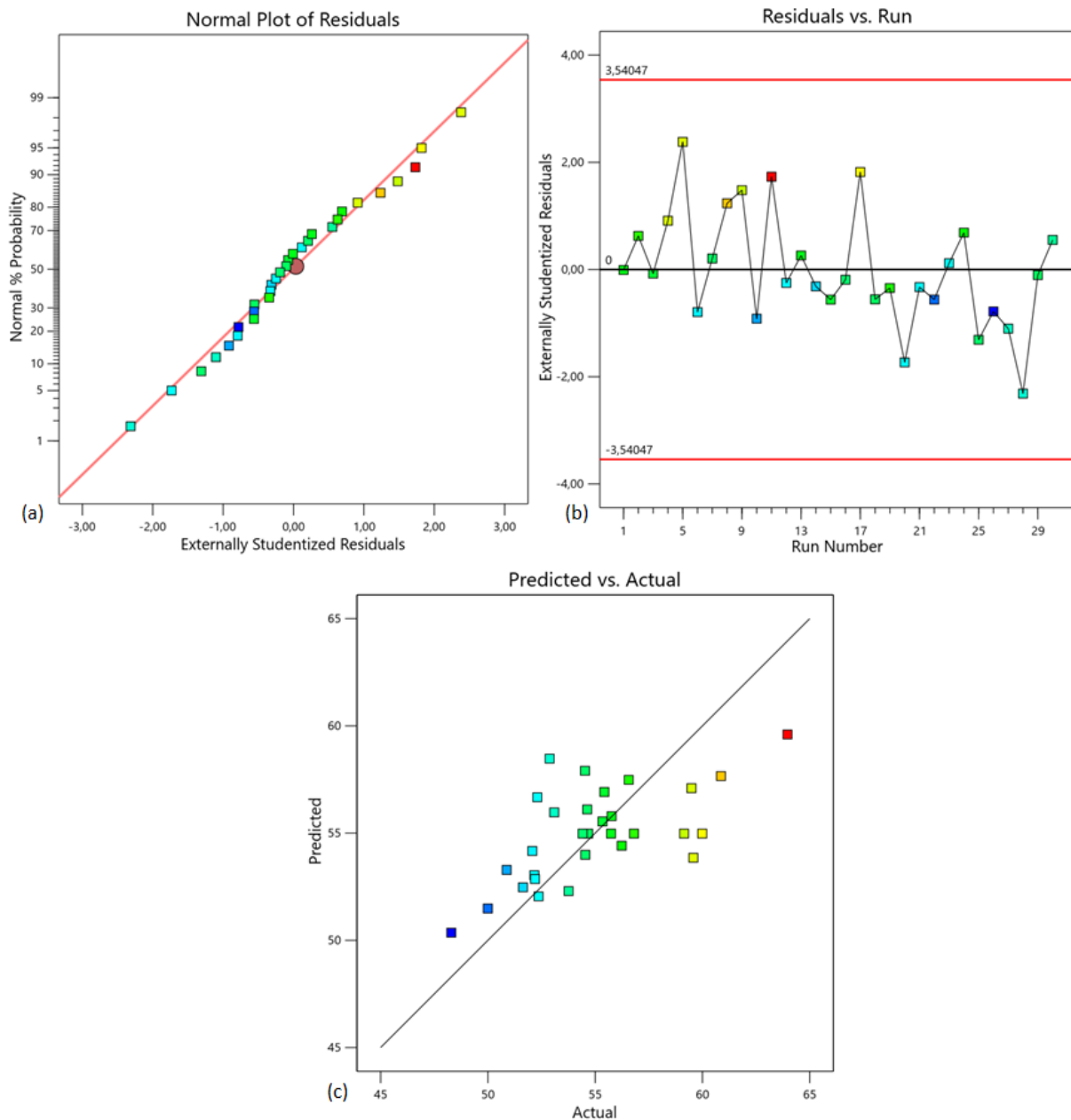


Figure 7 (a). Although the CS24h analysis indicates an adjusted  $R^2$  of 29.79%, which shows a low statistic, since ideally it should be close to 100%, the graph shows the 30 points very close to the straight line, obeying a linear pattern. Figure 8 (b) shows the residuals versus run plot and indicates that the student residuals are within the limit ( $\pm 3.54047$ ). However, its dispersion is on a downward trend and ideally it should be random. Also, one can find a bad behavior in points present in Figure 8 (c), in which some points are close to the line, others are already far away, with a tendency to be more centralized.



**Figure 8:** (a) Normal plot of Residuals CS24h; (b) Residuals versus Run plot for CS24h; and, (c) Predicted versus Actual plot for CS24h.

### 2.5. Model for Compressive Strength with 28 days (CS28d)

In the analysis of the results for 28-day compressive strength response model (CS28d), the best polynomial model was the linear one, with an adjusted  $R^2$  value of 26.22% and a predicted  $R^2$  of 8.71%. Even if the difference between these values is less than 20%, the model is significant, as it presents percentages far from 100%. When checking the diagnostic graphs, in order to find ways to adjust this model, for greater significance, the following behaviors were observed in Figure 9 (a), (b), (c) and (d):

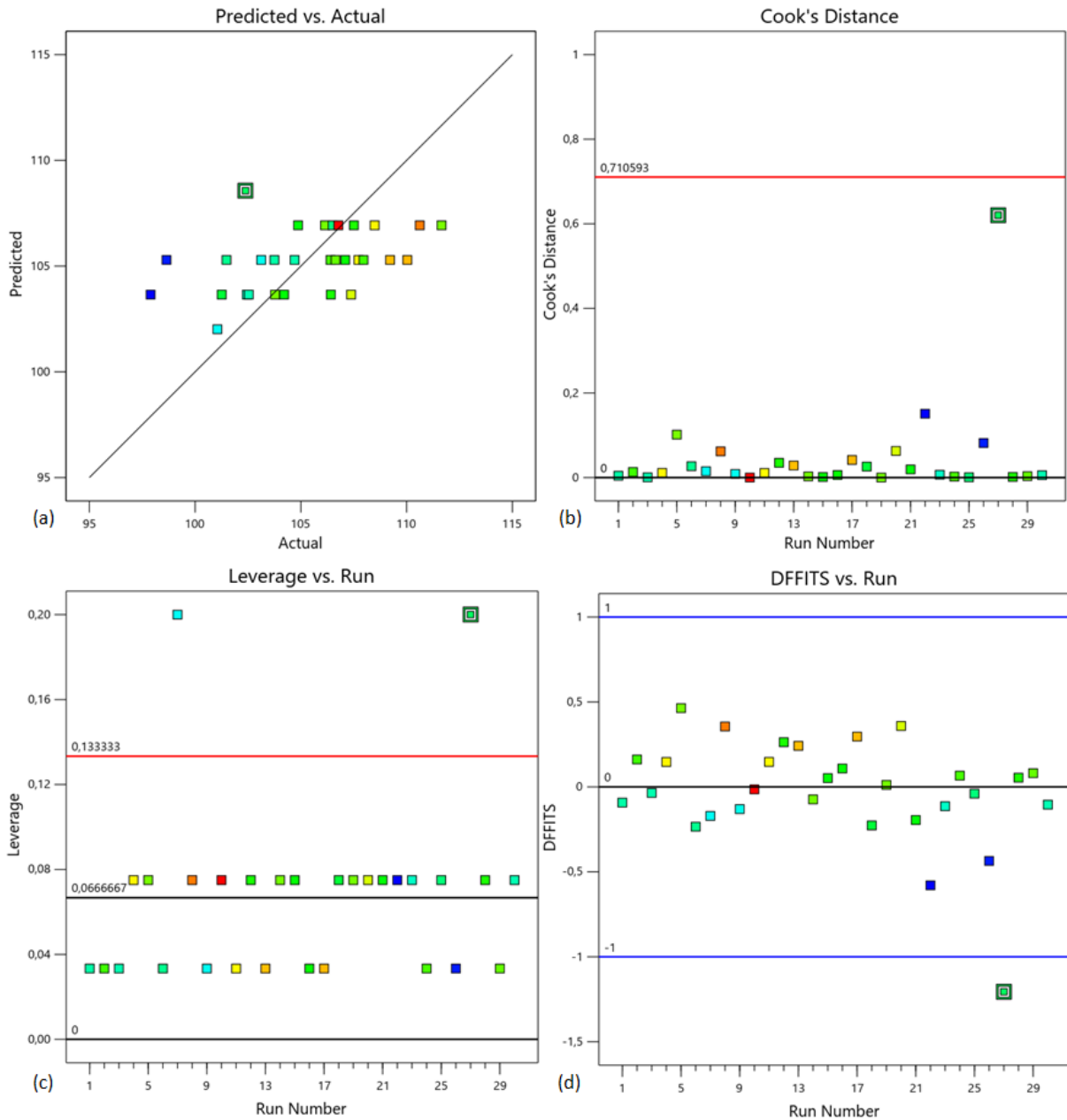


**Figure 9:** (a) Predicted versus Actual plot for CS28d; (b) Cook's Distance plot for CS28d; (c) Leverage versus Run plot for CS28d; e, (d) DFFITS versus Run plot for CS28d.

In Figure 9 (a) the graph has points distributed in the center with a horizontal tendency, characterizing little relationship between predicted versus actual. Still, it is not possible to find a specific point that could be harming the sample.

In Figure 10 (b), (c) and (d) that present Cook's Distance, Leverage versus Run and DFFITS versus Run, respectively, point to a common behavior: the positions in the graphs of point Std 23, Run 27. Figure 10 (b) this point is not an outlier, however, it is close to the limit (0.710593), far from the others. This implies that this single point is able to influence the estimate in a regression model.

Figure 10 (c), which demonstrates the leverage points, shows the student residue Std 23, Run 27, above the limit (0.133333), and is in a position above the double of the other points. This behavior is also valid for Figure 10 (d), which shows the DFFITS versus Run graph, in which the same point (Std 23, Run 27) is outside the limits (-1, 1). DFFITS presents the difference in fits,

which is a useful tool for detecting influential runs. In view of the analyses, the idea of ignoring Std 23, Run 27 and creating a new polynomial model is reinforced.

In Figure 9 (b), (c) and (d) that present Cook’s Distance, Leverage versus Run and DFFITS versus Run, respectively, its point to a common behavior: the positions in the graphs of point Std 23 Run 27. Figure 9 (b) this point is not an outlier, however, it is close to the limit (0.710593), in a distant position from the others. This implies that this single point is able to influence the estimate in a regression model.

Figure 9 (c) which demonstrates the leverage points, shows the student’s residual Std 23 Run 27, above the limit (0.133333), and is in a position above the double of the other points. This behavior is also valid for Figure 9 (d), which shows the DFFITS versus Run graph, in which the same point (Std 23 Run 27) is outside the limits (-1, 1). DFFITS presents the difference in fits, which is a useful tool for detecting influential runs. In view of the analyses, the idea of ignoring Std 23, Run 27 and creating a new polynomial model is reinforced.

After the new analysis, the linear model showed better results. The ANOVA for CS28d, present in Table 13, implies that the model is significant, with an “F-value” of 5.85 and a “p-value” of 0.002 (<0.05), that is, there are 0.2% chance of a high F-value occurs due to noise.

The significant model terms are the factors  $X_4$  (s/m) and  $X_1$  (w/c), respectively, in order of relevance. The terms  $X_2$  (Sp/p) and  $X_3$  (w/p) are insignificant, as they have values above 0.05. The lack of fit relative to pure error, with a value of 1.21, implies that it is not significant.

Source	Sum of Squares	Mean Square	F-value	p-value	Significance
<b>Model</b>	160.66	40.17	5.85	0.0020	significant
w/c	35.43	35.43	5.16	0.0323	
Sp/p	12.69	12.69	1.85	0.1865	
w/p	9.15	9.15	1.33	0.2597	
s/m	<b>103.40</b>	103.40	15.07	<b>0.0007</b>	
<b>Residual</b>	164.69	6.86			
Lack of Fit	135.22	7.12	1.21	0.4546	not significant
Pure Error	29.46	5.89			
<b>Cor Total</b>	325.35				

Table 13: ANOVA for CS28d.

Furthermore, there was a significant improvement in the determination coefficients for CS28d. In Table 14, the Predicted  $R^2$  value is 0.2732 and the Adjusted  $R^2$  is 0.4095, verifying a reasonable agreement between them, as the difference is less than 0.2. Even with coefficient increase, the Adjusted  $R^2$  is still far from 1.

In “Adeq. Precision”, the value is 8.9015, it has an adequate sign, because it has a desirable value greater than 4. Therefore, this model is suitable for navigating the design space.

Std. Dev.	Mean	C.V.%	$R^2$	Ajusted $R^2$	Predicted $R^2$	Adeq Precision
2.62	105.39	2.49	0.4938	0.4095	0.2732	<u>8.9015</u>

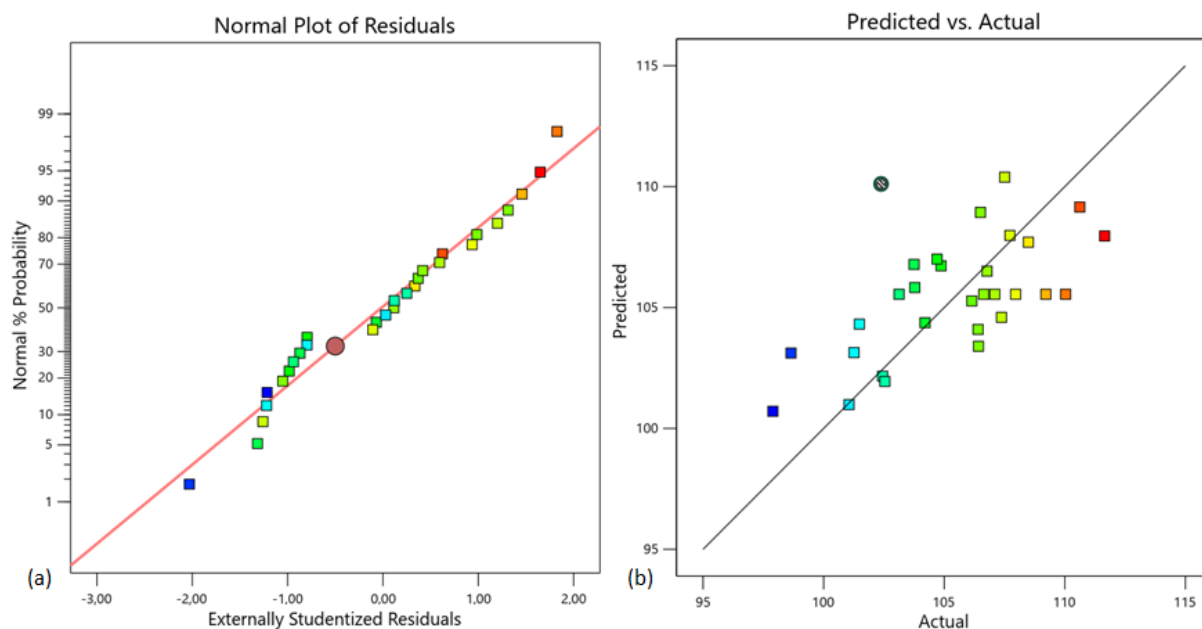
Table 14: Fit statistics for CS28d.

Table 15 shows the estimated coefficient for each response variable, the standard error and the 95% confidence intervals. In addition, it presents the VIFs, being orthogonal factors (equal to 1), and as a rule, the VIFs are considered tolerable (< 10).

Factor	Coefficient Estimate	Standard Error	95% CI Low	95% CI High	VIF
Intercept	105.5500	0.4881	104.54	106.56	
w/c	-1.2100	0.5347	-2.32	-0.11	1.0000
Sp/p	0.7272	0.5347	-0.38	1.83	1.0000
w/p	0.6173	0.5347	-0.49	1.72	1.0000
s/m	-2.2800	0.5878	-3.49	-1.07	1.0000

**Table 15:** Coefficients in Terms of Coded Factors – CS28d.

The plot of normal versus residuals are shown in Figure 10 (a) after point Std 23 Run 27 is skipped. Student residuals are close to the line, showing characteristics with a linear trend. The graph of Figure 10 (b), which shows the predicted versus actual relationship, when compared with the previous graph (without ignoring the point Std 23 Run 27) it shows an improvement in the distribution of the points around the line and smaller dispersions. The location of point Std 23 Run 27, which was disregarded, can be seen in the graph.



**Figure 10:** (a) Normal plot of Residuals CS28d; and, (b) Predicted versus Actual plot for CS28d.

## 2.6. Optimization of self-compacting mortars

The experimental planning aims to optimize the mixtures in order to obtain a better efficient composition for a given objective. In each of the responses, a model was developed. Numerical optimization was carried out using the Design Expert software in order to find a mixture that causes less impact on the environment and costs, in addition to obtaining better results regarding segregation and compression strength.

The parameters for optimization are defined as “goal” to build desirability indices. They are: maximize, minimize, targeted, in range and equal to. In addition, weights ranging from 0.1 to 10 are defined, with a default value of 1. And finally, the degree of importance, which is a tool that serves to determine the factors that are priorities to achieve the established goals. Importance levels range from 1 plus (+) to 5 plus (++++). Therefore, a set of conditions is randomly calculated to look for desirable results. Initially, individual objectives are combined and then the general desire (Myers, Montgomery, and Anderson-cook 2009).

The parameters defined for the optimization of self-compacting mortar, aiming to obtain lower environmental impacts, lower costs, reduce segregation and higher compressive strength are observed in Table 16:

Name	Goal	Lower Limit	Upper Limit	Importance
$X_1$ : w/c	maximize	0.841097	0.948471	5
$X_2$ : Sp/p	minimize	0.0220967	0.0249176	4
$X_3$ : w/p	is in range	0.501287	0.565281	3
$X_4$ : s/m	maximize	0.4512	0.5088	5
$Y_1$ : D-Flow	is target = 328	289	367	3
$Y_2$ : T-Funnel	maximize	11.45	66.78	4
$Y_3$ : CS24h	is in range	48.2929	63.9652	3
$Y_4$ : CS28d	maximize	105	111.654	5

**Table 16:** Defined criteria for optimizing self-compacting mortar.

The input factor  $X_1$  (w/c) aimed to maximize its result, considering a lower water/cement ratio and consequently a smaller amount of cement, reducing the environmental impact from the cement manufacturing process and the  $CO_2$  emission. In addition, reducing the amount of cement promotes the reduction of costs of this mixture. The degree of importance defined was 5.

The goal of the variable  $X_2$  (Sp/p) was to minimize it in order to reduce costs with a superplasticizer additive, with a degree of importance 4. For the variable  $X_3$  (w/p) it was only defined that it should be between the limit intervals, because for this optimization, this factor is of little relevance. By maximizing the input factor  $X_4$  (s/m), it meets the same criteria as the input factor  $X_1$ , as it increases the sand/mortar ratio, reducing costs and the environmental impact of the mixture, as it will have a lower percentage of cement.

For the response variable  $Y_1$  (D-Flow), an average value (328 mm) was defined as the goal, aiming at better responses for segregation. As for the response  $Y_2$  (T-Funnel), also to avoid segregation, higher values are recommended, so it was maximized with a degree of importance 4. For the third response variable  $Y_3$  (CS24h), only obeying the intervals was used as a criterion parameter, with degree of importance 3, bearing in mind that it is of little relevance to reach minimum or maximum values of strength in 24 hours for the established objectives.

Finally, there is the response variable  $Y_4$  (CS28d) whose optimization criterion was maximization, with a degree of importance 5, and a minimum limit value of 105 MPa. The objective was to make the mixture optimized with higher compressive strength values at 28 days.

For the optimization criteria defined above, 65 mixes were found that meet the targets. Table 17 lists the 10 best mixing solutions, highlighting for number 1. The best result found for optimization, with a degree of accuracy of 95%, is shown in Table 18. The values found followed the established criteria and solution 1 is the one with the best mix from an economic and environmental point of view and fresh and hardened properties.

Number	w/c	Sp/p	w/p	s/m	d-flow	t-funnel	CS24h	CS28d	Desirability	Significance
1	0.902	0.023	0.561	0.464	349.443	17.819	55.193	106.922	0.428	Selected
2	0.898	0.023	0.558	0.477	341.301	20.782	55.016	105.689	0.418	
3	0.907	0.023	0.537	0.468	341.220	21.420	54.626	106.051	0.413	

4	0.934	0.022	0.559	0.464	353.686	16.136	53.699	105.882	0.409
5	0.930	0.024	0.555	0.472	347.821	17.970	53.981	106.043	0.407
6	0.928	0.023	0.538	0.464	347.133	18.770	53.873	106.147	0.399
7	0.939	0.023	0.552	0.463	352.751	16.509	53.424	105.780	0.395
8	0.899	0.023	0.547	0.480	336.702	23.104	54.922	105.633	0.395
9	0.937	0.023	0.546	0.462	351.455	17.073	53.644	106.271	0.394
10	0.900	0.023	0.521	0.467	336.488	24.386	54.751	106.018	0.393

**Table 178:** 10 best blending solutions found for optimization.

Solution 1 of 65 Response	Predicted Mean	Predicted Median*	Std Dev	SE Pred	95% PI low	95% PI high
Y <sub>1</sub> : D-Flow	349.4430	349.4430	8.96135	9.30649	330.2760	368.6100
Y <sub>2</sub> : T-Funnel	17.4195	3.0964	3.09643	N/A	12.3651	26.3489
Y <sub>3</sub> : CS24h	55.1935	55.1935	2.92905	3.04727	48.9175	61.4694
Y <sub>4</sub> : CS28d	106.9220	106.9220	2.61952	2.73513	101.2770	112.5680

**Table 18:** Confirmation of the best optimized result.

### 3. Conclusion

The research carried out aimed to investigate the input variables for a self-compacting mortar, in order to allow the models to be adapted to its properties. In addition, the mixture was optimized by establishing economic, environmental and fresh and hardened criteria, using the response surface methodology (RSM). Based on the results found, the following conclusions are explained:

1. In the preliminary analyzes, the T-funnel versus D-Flow and D-Flow versus T-funnel ratio already showed a strong descending correlation of -0.871;
2. The D-flow and T-funnel linear polynomial models were adequate to relate to the self-compacting mortar;
3. Linear polynomial models CS14h and CS28d were of moderate significance for the self-compacting mortar. Adjustments will be needed to provide better results;
4. For the D-Flow and T-Funnel responses, the w/p, s/m and w/c factors had the most significant effects;
5. The CS24h response variable was more influenced by the w/c factor;
6. The w/c and s/m factor were more significant for CS28d;
7. The numerical optimization solutions showed high compliance, with good precision, emphasizing the efficiency of RSM for mixture optimization;
8. The criteria defined for model optimization allowed finding solutions for the established objectives.

## Acknowledgments

This work is financially supported by: Base Funding –UIDB/04708/2020 of the CONSTRUCT – Instituto de I&D em Estruturas e Construções - funded by national funds through the FCT/MCTES (PIDDAC). This work is funded by national funds through FCT –Fundação para a Ciência e a Tecnologia, I.P., under the Scientific Employment Stimulus –Institutional Call – CEECINST/00049/2018.

## References

- Aitcin, P. C. 2000. *Concreto De Alto Desempenho*. Edited By Pini. 1 Ed. São Paulo.
- Ali, Mujahid, Muhammad Imran Khan, Faisal Masood, Badr T. Alsulami, Belgacem Bouallegue, Rab Nawaz, And Roman Fediuk. 2022. “Central Composite Design Application In The Optimization Of The Effect Of Waste Foundry Sand On Concrete Properties Using Rsm.” *Structures* 46 (December): 1581–94. <https://doi.org/10.1016/j.istruc.2022.11.013>.
- Ali, Mujahid, Abhinav Kumar, A. Yvaz, And Bashir Salah. 2023. “Central Composite Design Application In The Optimization Of The Effect Of Pumice Stone On Lightweight Concrete Properties Using Rsm.” *Case Studies In Construction Materials* 18 (July): E01958. <https://doi.org/10.1016/j.cscm.2023.E01958>.
- Anurag, And S. K. Singh. 2022. “Estimation Of The Impacts Of Adding Recycled Demolition Waste And Steel Fibers On Different Mechanical Properties Of Self-Compacting Concrete.” *Materials Today: Proceedings* 48 (January): 1723–30. <https://doi.org/10.1016/j.matpr.2021.10.031>.
- Box, G. E. P.; Hunter, W. G.; Hunter, J. S. 1978. *Statistics For Experimenters: An Introduction To Design, Data Analysis And Model Building*. Edited By Wiley. New York.
- Box, G. E. P.; Wilson, K. B. 1951. “On The Experimental Attainment Of Optimum Conditions.” *J. Royal Statistic Soc.*, 1–38.
- Calado, Carlos Fernando De Araújo, Aires Camões, Said Jalali, And Béda Barkokébas Junior. 2015. *Concreto Auto-Adensável (Caa), Mais Do Que Alternativa Ao Concreto Convencional (Cc)*. Edited By Editora Universidade De Pernambuco - Edupe. Recife.
- Coz Diaz, Juan Jose Del, Paulino Jose Garcia-Nieto, Felipe Pedro Alvarez-Rabanall, Mar Alonso-Martínez, Javier Dominguez-Hernandez, And Jose Maria Perez-Bella. 2014. “The Use Of Response Surface Methodology To Improve The Thermal Transmittance Of Lightweight Concrete Hollow Bricks By Fem.” *Construction And Building Materials* 52 (February): 331–44. <https://doi.org/10.1016/j.conbuildmat.2013.11.056>.
- Day, R., Holton, I., Domone, P., & Bartos, P. 2005. “Self-Compacting Concrete: A Review.” *Concrete Society*, No. 62.
- En. 2016. “Bs En 196-1:2016 - Methods Of Testing Cement: Determination Of Strength.”
- Ferdosian, Iman, And Aires Camões. 2017. “Eco-Efficient Ultra-High Performance Concrete Development By Means Of Response Surface Methodology.” *Cement And Concrete Composites* 84 (November): 146–56. <https://doi.org/10.1016/j.cemconcomp.2017.08.019>.
- Ghafari, Ehsan, Hugo Costa, And Eduardo Júlio. 2014. “Rsm-Based Model To Predict The Performance Of Self-Compacting Uhcp Reinforced With Hybrid Steel Micro-Fibers.” *Construction And Building Materials* 66 (September): 375–83. <https://doi.org/10.1016/j.conbuildmat.2014.05.064>.
- Imran Khan, Muhammad, Muslich H Sutanto, Madzlan B Napih, Muhammad Zahid, And Aliyu Usman. 2020. “Optimization Of Cementitious Grouts For Semi-Flexible Pavement Surfaces



- Using Response Surface Methodology.” *Iop Conference Series: Earth And Environmental Science* 498 (1): 012004. <https://doi.org/10.1088/1755-1315/498/1/012004>.
- Keleştemur, Oğuzhan, Servet Yildiz, Bihter Gökçer, And Erdinç Arici. 2014. “Statistical Analysis For Freeze–Thaw Resistance Of Cement Mortars Containing Marble Dust And Glass Fiber.” *Materials & Design* 60 (August): 548–55. <https://doi.org/10.1016/j.matdes.2014.04.013>.
- Khan, Muhammad Imran, Muslich Hartadi Sutanto, Madzlan Bin Napiah, Kaffayatullah Khan, And Waqas Rafiq. 2021. “Design Optimization And Statistical Modeling Of Cementitious Grout Containing Irradiated Plastic Waste And Silica Fume Using Response Surface Methodology.” *Construction And Building Materials* 271 (February): 121504. <https://doi.org/10.1016/j.conbuildmat.2020.121504>.
- Maia, Lino. 2022. “Experimental Dataset From A Central Composite Design With Two Qualitative Independent Variables To Develop High Strength Mortars With Self-Compacting Properties.” *Data In Brief* 40 (February): 107738. <https://doi.org/10.1016/j.dib.2021.107738>.
- Matos, Ana Mafalda, Lino Maia, Sandra Nunes, And Paula Milheiro-Oliveira. 2018. “Design Of Self-Compacting High-Performance Concrete: Study Of Mortar Phase.” *Construction And Building Materials* 167 (April): 617–30. <https://doi.org/10.1016/j.conbuildmat.2018.02.053>.
- Mermerdaş, Kasım, Zeynep Algin, Safie Mahdi Oleiwi, And Dia Eddin Nassani. 2017. “Optimization Of Lightweight Ggbfs And Fa Geopolymer Mortars By Response Surface Method.” *Construction And Building Materials* 139 (May): 159–71. <https://doi.org/10.1016/j.conbuildmat.2017.02.050>.
- Mohammed, Bashar S., Ong Chuan Fang, Khandaker M. Anwar Hossain, And Mohamed Lachemi. 2012. “Mix Proportioning Of Concrete Containing Paper Mill Residuals Using Response Surface Methodology.” *Construction And Building Materials* 35 (October): 63–68. <https://doi.org/10.1016/j.conbuildmat.2012.02.050>.
- Moraes, K. A. M. 2010. “Otimização Do Uso De Adições Mineraias Para A Produção De Concreto Auto-Adensável.” Universidade Federal De Pernambuco.
- Myers, R. H., D. C. Montgomery, And C.M. Anderson-Cook. 2009. *Response Surface Methodology*. Edited By John Wiley & Sons. 3rd Editio. New York.
- Neto, B. De B.; Scarminio, I. S.; Bruns, R. E. 2001. *Como Fazer Experimentos: Pesquisa E Desenvolvimento Na Ciência E Na Indústria*. Edited By Editora Unicamp. 2° Ed. Campinas, Sp.
- Nunes, S. C. B. 2001. “Betão Auto-Compactável: Tecnologia E Propriedades.” Universidade Do Porto.
- Nunes, Sandra, Ana Mafalda Matos, Tiago Duarte, Helena Figueiras, And Joana Sousa-Coutinho. 2013. “Mixture Design Of Self-Compacting Glass Mortar.” *Cement And Concrete Composites* 43 (October): 1–11. <https://doi.org/10.1016/j.cemconcomp.2013.05.009>.
- Nuruzzaman, Md, Tajkia Ahmad, Prabir Kumar Sarker, And Faiz Uddin Ahmed Shaikh. 2023. “Rheological Behaviour, Hydration, And Microstructure Of Self-Compacting Concrete Incorporating Ground Ferronickel Slag As Partial Cement Replacement.” *Journal Of Building Engineering* 68 (June): 106127. <https://doi.org/10.1016/j.job.2023.106127>.
- Okamura, H.; Ouchi, M. 2003. “Self-Compacting Concrete.” *Journal Of Advanced Concrete Technology* 1 (1): 5–15.

- Okamura, H. 1997. "Self-Compacting High Performance Concrete." *Concrete International* 19 (7): 50–54.
- Salaheen, M.; Alaloul, W.S.; Malkawi, A.B.; De Brito, J.; Alzubi, K.M.; Al-Sabaei, A.M.; Alnarabiji, M.S. Al. 2022. "Modelling And Optimization For Mortar Compressive Strength Incorporating Heat-Treated Fly Oil Shale Ash As An Effective Supplementary Cementitious Material Using Response Surface Methodology." *Materials* 15 (19). <https://doi.org/10.3390/ma15196538>.
- Shi, Xiaoshuang, Cong Zhang, Xiaoqi Wang, Tao Zhang, And Qingyuan Wang. 2022. "Response Surface Methodology For Multi-Objective Optimization Of Fly Ash-Ggbs Based Geopolymer Mortar." *Construction And Building Materials* 315 (January): 125644. <https://doi.org/10.1016/j.conbuildmat.2021.125644>.
- Stat-Ease. 2014. *Handbook For Experimenters. Version 11.* [http://www.statease.com/pubs/handbk\\_for\\_exp\\_sv.pdf](http://www.statease.com/pubs/handbk_for_exp_sv.pdf).
- Upasani, R.; Banga, S.; Ajay, K. 2004. "Response Surface Methodology To Investigate The Iontophoretic Delivery Of Tacrine Hydrochloride." *Pharm Res.* 21: 2293–99. <https://doi.org/10.1007/s11095-004-7682-6>.
- Waqar, Ahsan, Naraindas Bheel, Hamad R. Almujiabah, Omrane Benjeddou, Mamdooh Alwetaishi, Mahmood Ahmad, And Mohanad Muayad Sabri Sabri. 2023. "Effect Of Coir Fibre Ash (Cfa) On The Strengths, Modulus Of Elasticity And Embodied Carbon Of Concrete Using Response Surface Methodology (Rsm) And Optimization." *Results In Engineering* 17 (March): 100883. <https://doi.org/10.1016/j.rineng.2023.100883>.
- Zahid, Muhammad, Nasir Shafiq, M. Hasnain Isa, And Lluís Gil. 2018. "Statistical Modeling And Mix Design Optimization Of Fly Ash Based Engineered Geopolymer Composite Using Response Surface Methodology." *Journal Of Cleaner Production* 194 (September): 483–98. <https://doi.org/10.1016/j.jclepro.2018.05.158>.
- Zerbino, R., B. Barragán, T. Garcia, L. Agulló, And R. Gettu. 2009. "Workability Tests And Rheological Parameters In Self-Compacting Concrete." *Materials And Structures/Materiaux Et Constructions* 42 (7): 947–60. <https://doi.org/10.1617/S11527-008-9434-2/Figures/6>.